Chinese Herbal Medicines 12 (2020) 195–199

Contents lists available at ScienceDirect

Chinese Herbal Medicines

journal homepage: www.elsevier.com/locate/chmed

Original Article

Chemical constituents from acid hydrolyzates of *Panax quinquefolius* total saponins and their inhibition activity to α-glycosidase and protein tyrosine phosphatase 1B

Si-wen Han[a], Sheng-ming Shi[b], Yu-xiao Zou[a], Zhi-cheng Wang[c], Yan-qun Wang[a,d], Lin Shi[a,d,*], Ting-cai Yan[a,*]

[a] College of Food Science, Shenyang Agricultural University, Shenyang 110866, China
[b] Tianjin Press of Chinese Herbal Medicines, Tianjin Institute of Pharmaceutical Research, Tianjin 300462, China
[c] Dalian Institute for Drug Control, Dalian 116021, China
[d] Key Laboratory of Healthy Food Nutrition and Innovative Manufacturing of Liaoning Province, Shenyang Agricultural University, Shenyang 110866, China

ARTICLE INFO

Article history:
Received 3 December 2019
Revised 23 January 2020
Accepted 5 February 2020
Available online 14 March 2020

Keywords:
Panax quinquefolius L.
total saponins
acid hydrolysis
hypoglycemic effect

ABSTRACT

Objective: To investigate the hypoglycemic components from the acid hydrolyzates of *Panax quinquefolius* total saponins, and screen the active compounds by *in vitro* inhibitory activities to α-glycosidase enzymes and protein tyrosine phosphatase-1B (PTP1B).
Methods: The hydrolyzates were chromatographed repeatedly over silica gel column, and the structures of the compounds were determined by means of NMR. The *in vitro* bioassay was performed through the inhibitory effects on α-glucosidase or/and PTP1B.
Results: Eight compounds were isolated, which identified as 20(*S*)-panaxadiol (**1**), (20*S*,24*R*)-dammarane-20,24-epoxy-3β,6α,12β,25-tetraol (**2**), 20(*R*)-dammarane-3β,12β,20,25-tetraol (**3**), 20(*S*)-dammarane-3β,6α,12β,20,25-pentol (**4**), 20(*R*)-dammarane-3β,12β,20,25-tetrahydroxy-3β-*O*-β-*D*-glucopyranoside (**5**), β-sitosterol (**6**), oleanolic acid (**7**) and 20(*S*)-protopanaxadiol (**8**). Compound **5** was ginseng triterpenoid isolated from the acid hydrolysates of total saponins from *P. quinquefolius* for the first time. In this paper, the possible *in vitro* inhibitory activities were investigated. Compound **5** exhibited significantly inhibitory activity against α-glucosidase, and the IC_{50} value [(0.22 ± 0.21) μmol/L] was about 43-fold lower than positive control. For the PTP1B inhibition assay, compound **5** indicated the strongest inhibitory effect with IC_{50} of (5.91 ± 0.38) μmol/L, followed by compound **4** with IC_{50} of (6.21 ± 0.21) μmol/L, which were all showed competitive inhibitory pattern by using a Lineweaver-Burk plot.
Conclusion: These results supported the potential application of dammaranes from acid hydrolyzates of *P. quinquefolius* total saponins can be used as ingredients of ancillary anti-diabetic agent or functional factor.

1. Introduction

Diabetes mellitus (DM) is one of the major global public health problems, which describes a group of metabolic disorders characterized by high blood glucose levels. Its prevalence is currently increasing at an alarming rate (Cho et al., 2018). Type 2 diabetes is complicated metabolic disorder arising from insulin deficiency, or/and insulin resistance (Imam, 2012). Lots of researches on development of effective hypoglycaemic methods have provided discoveries of molecular therapy targets, such as α-glucosidase and protein tyrosine phosphatase-1B (PTP1B) (Fang, Cao, Duan, Tang, & Zhao, 2014). Recently, an increased interest in bioactive natural products by scientists, as a source of potential anti-diabetic agents, has been observed.

Panax quinquefolius L., also called American ginseng, is widely distributed in North America and cultivated in China, which has been traditionally used as a tonic with prophylactic and restorative properties. And the biologically active constituents are dammarane-type glycosides (Liu et al., 2013; Wang et al., 2001), with beneficial effects reported about treatment of type 2 diabetes

* Corresponding authors.
E-mail addresses: linnashi@126.com (L. Shi), ytc126127@163.com (T.-c. Yan).

https://doi.org/10.1016/j.chmed.2020.03.003

mellitus (Vuksan et al., 2000), anticancer (Qi, Wang, & Yuan, 2010) and immunopotentiating.

As a continuation of our work for discovering more effective components, this paper focused on the isolation of triterpenoids from the acid hydrolyzates of *P. quinquefolius* total saponins and their inhibitory activities of α-glucosidase and PTP1B were evaluated.

2. Materials and methods

2.1. General

Melting points were determined with the X-4 Electrothermal melting point apparatus (Taike, Beijing) and are uncorrected. NMR Spectra were obtained from Bruker AV-600 and ARX-400 spectrometers using TMS as internal standard. The 96-well microplate reader was from Microplate Reader (imark, BIORAD, USA). Silica gel (Qingdao Marine Chemical Co., Ltd, China) were used for TLC and column chromatography.

2.2. Plant material and reagents

The crude saponins of *P. quinquefolius* (> 80%) were purchased from Longpu Bio-Tech Inc., Liaoning Province, China.

PTP1B (human, recombinant), yeast α-glucosidase, $NaVO_4$, acarbose, dithiothreitol (DTT), pnitrophenyl-α-D-glucopyranoside (pNPG), p-nitrophenyl phosphate (pNPP), β-mercaptoethanol were purchased from Sigma-Aldrich. Ethanol, dichloromethane, petroleum ether, acetone, HCl, Na_2CO_3 and other chemicals of analytical grade were from Shenyang Factory of Chemicals, China.

2.3. Extraction and isolation

According to the acid hydrolysis method reported (Bai et al., 2010), the hydrolyzates (30 g) were isolated from the total saponins of *P. quinquefolius*. The extract was chromatographed repeatedly over silica gel column with petroleum ether-acetone (100:0–0:100, volume percent) to provide five fractions A–E. Fraction B (2.5 g) was separated into eight fractions, frs. B_a–B_h. Compound **1** (20 mg) was afforded from B_c (petroleum ether: acetone 100:10). Compounds **2** (30 mg), **3** (20 mg) and **4** (40 mg) were afforded from B_e (petroleum ether: acetone 100:15). Compounds **6** (30 mg), **7** (35 mg) and **8** (25 mg) were gained from B_g (petroleum ether: acetone 100:25). Fraction D (0.8 g) was purified on silica gel column eluted with petroleum ether-acetone to afford compound **5** (20 mg) from subfraction 8 (100:40).

2.4. Assay for α-glycosidase inhibitory activity

The α-glucosidase inhibitory activities were determined following the modified method (Tao, Zhang, Cheng, & Wang, 2013), using a 96-well plate with PNPG as the substrate. A total of 30 μL of the enzyme solution (2 U/mL α-glucosidase in potassium phosphate buffer, pH 6.8) and 20 μL of each compound (in 1% DMSO) at various concentrations were mixed, and incubated at 37.0 °C for 5 min, subsequently. The reaction was started when 150 μL of pNPG (10 mmol/L) and 800 μL of 0.1 mol/L potassium phosphate buffer were added. After incubation for 30 min, 2 mL of 1 mol/L Na_2CO_3 in potassium phosphate buffer was added to stop the reaction. The blank control group was added 20 μL of 1% DMSO instead of the sample solution. The amount of PNP released was quantified by the absorbance at 405 nm.

2.5. Assay for PTP1B inhibitory activity

The method of PTP1B inhibition assay was conducted as previously reported method (Xu, Cao, Yue, Zhang, & Zhao, 2018). The different concentrations (in 1% DMSO) of all compounds were tested, and $NaVO_4$ was used as a positive control. Totally, 10 μL of test samples (5, 25, 50, 75, 150 μmol/L), 83 μL enzyme in buffer (pH7.5) and 4 μL pNPP in reaction system pH 7.5, 2 mmol/L EDTA, 100 mmol/L NaCl, 1 m mol/L LDTT and tendency for 50 mmol/L Tris–HCl were mixed at 37 °C for 30 min, and 5 μL NaOH (2 mmol/L) was added to stop the reaction. At 405 nm, dephosphorylation of pNPP generated product pNP can be measured (Xiao, Guo, Sun, & Zhao, 2017).

2.6. Kinetic of α-glucosidase and PTP1B inhibitions

Compound **5** was analyzed for inhibitory type against α-glucosidase and PTP1B. The methods were measured as previously reported by Xu et al. (2018). The reaction mixture consisted of different concentrations of pNPG (or pNPP) as a substrate in the absence or presence of compound **5** at different concentrations. Concentration of inhibitors was fixed at 0, 5, 20 and 60 μmol/L (0, 25, 50 and 75 μmol/L), while concentration of substrate was varied at 0.125, 0.2, 0.25, 0.33, 0.5, and 1.0 mmol/L (or 0.2, 0.25, 0.33, 0.5, 1.0, and 2.0 mmol/L). According to Lineweave–Burk method, 1/[S] was used as the horizontal coordinate and 1/V as the vertical coordinate to plot the inhibition kinetics curves of compound **5**, and we analyzed to determine the type of inhibition.

2.7. Molecular docking study

To investigate the interaction between compound **5** and PTP1B, the active site analysis method was carried out in molecular docking study. The crystal structure of PTP1B (PDB ID 2QBQ) was obtained from the Protein Data Bank (PDB) online. The structure optimization of compound **5** was processed by ChemBioDraw, and the docking calculation was performed using Schrodinger Suite 2009 software package installed on Dell Precision TM T5500 workstation. The operating system was Red Head Enterprise Linux server 5.0. Molecular docking analysis and mapping were performed by Discovery Studio Visualizer 3.5 and PyMOL (DeLano Scientific). Blind docking of **5** to the catalytic active site (site A, residues 214–221) of PTP1B and the secondary lipophilic non-catalytic aryl phosphate ester binding site (site B) was investigated.

2.8. Statistical analysis

Data were statistically treated by analysis of variance using SPSS 16.0 software. All data was expressed as mean ± S.D. in triplicate, $P < 0.05$ was considered statistically significant.

3. Results and discussion

3.1. Structural identification of compounds 1–8

3.1.1. 20(S)-panaxadiol (*1*)

White crystals. Mp 239–241 °C. ESI-MS *m/z*: 459.5 $[M-H]^-$. ^{1}H NMR (400 MHz, C_5D_5N) δ: 5.32 (1H, t, J = 7.2 Hz, H-24), 3.91 (1H, m, H-12α), 3.43 (1H, m, H-3α), 1.59 (3H, s, H-28), 1.46 (3H, s, H-21), 1.27 (3H, s, H-26), 1.23 (3H, s, H-27), 1.22 (3H, s, H-18), 1.03 (3H, s, H-29), 0.99 (3H, s, H-19), 0.88 (3H, s, H-30). ^{13}C NMR data (100 MHz, C_5D_5N) see Table 1.

3.1.2. (20S,24R)-dammarane-20,24-epoxy-3β,6α,12β,25- tetraol (*2*)

White crystals. Mp 199–201 °C. ESI-MS *m/z*: 493.4 $[M + H]^+$. ^{1}H NMR (400 MHz, C_5D_5N) δ: 4.40 (1H, m, H-6β), 3.74 (1H, m, H-12α), 3.53 (1H, m, H-3α), 1.98 (3H, s, H-28), 1.51 (3H, s, H-21), 1.46 (3H, s, H-26), 1.33 (6H, s, H-18, H-27), 1.09 (3H, s, H-29), 1.00 (3H, s, H-19), 0.95 (3H, s, H-30). ^{13}C NMR data (100 MHz, C_5D_5N) see Table 1.

Table 1
^{13}C NMR (100 MHz or 150 MHz) data of compounds **1**–**8** in C_5D_5N.

NO.	1	2	3	4	5	6	7	8
1	39.6	39.4	39.6	39.1	39.2	30.1	38.7	39.4
2	28.3	28.1	28.3	27.9	28.2	31.8	27.9	28.3
3	78.1	78.4	78.0	78.2	88.8	71.7	77.8	78.0
4	39.5	40.4	39.4	40.1	39.7	41.9	39.2	39.6
5	56.4	61.9	56.4	61.6	56.4	140.9	55.6	56.4
6	18.8	67.7	18.8	67.5	18.5	121.8	18.6	18.8
7	35.3	47.5	35.3	47.3	35.2	30.0	33.0	35.2
8	40.1	41.1	40.1	41.0	40.1	31.9	39.5	40.1
9	50.3	50.5	50.5	49.9	50.4	50.8	47.9	50.5
10	37.4	39.4	37.4	39.1	37.0	37.8	37.1	37.3
11	31.4	32.4	32.2	31.2	32.2	22.7	23.5	32.1
12	70.3	71.2	70.9	70.8	70.9	37.2	122.3	71.0
13	49.9	48.4	49.3	48.1	49.3	44.0	144.6	48.6
14	51.4	52.1	50.8	51.4	50.8	56.5	41.9	51.7
15	31.3	31.7	31.5	31.9	31.5	27.7	28.1	31.4
16	25.4	25.5	26.7	26.6	26.7	27.3	23.6	26.9
17	55.0	49.4	51.8	54.5	51.8	58.3	46.4	54.8
18	17.3	17.8	16.5	17.2	16.8	20.7	41.8	16.3
19	16.5	17.2	17.4	16.8	17.4	23.1	46.3	15.9
20	76.9	86.7	73.4	73.1	73.3	36.0	30.7	72.9
21	19.7	27.0	22.9	27.0	22.9	19.4	34.0	27.1
22	35.8	32.8	44.1	36.3	44.1	33.9	33.0	35.9
23	16.5	28.8	18.8	18.9	18.8	29.9	28.6	23.0
24	36.6	85.6	45.6	45.5	45.6	46.0	16.3	126.3
25	73.1	70.4	69.7	69.4	69.7	25.7	15.3	130.7
26	33.2	27.2	30.0	29.7	30.0	12.2	17.2	25.8
27	27.4	27.7	30.3	30.0	30.2	31.7	25.9	17.6
28	28.7	31.9	28.7	31.7	26.8	21.0	180.0	28.7
29	15.9	16.5	15.9	16.3	15.9	21.0	33.0	16.4
30	16.4	18.4	16.4	17.3	16.4		23.5	17.0
glc-1′					107.0			
2′					75.8			
3′					78.8			
4′					71.9			
5′					78.4			
6′					63.1			

*3.1.3. 20(*R*)-dammarane-3β,12β,20,25-tetraol (**3**)*

White crystals. Mp 251–253 °C. ESI-MS *m/z*: 477.7 $[M-H]^-$. ^1H NMR (400 MHz, C_5D_5N) δ: 3.94 (1H, m, H-12α), 3.43 (1H, m, H-3α), 1.44 (9H, s, H-26, 27, 28), 1.07 (3H, s, H-21), 1.05 (3H, s, H-18), 1.04 (3H, s, H-29), 0.93 (3H, s, H-19), 0.94 (3H, s, H-30). ^{13}C NMR data (100 MHz, C_5D_5N) see Table 1.

*3.1.4. 20(S)-dammarane-3β,6α,12β,20,25-pentol (**4**)*

White crystals. Mp 247–249 °C. ESI-MS *m/z*: 493.6 $[M-H]^-$. ^1H NMR (400 MHz, C_5D_5N) δ: 4.41 (1H, m, H-6β), 3.94 (1H, m, H-12α), 3.53 (1H, m, H-3α), 1.99 (3H, s, H-28), 1.45 (3H, s, H-21), 1.42 (3H, s, H-26), 1.39 (3H, s, H-27), 1.38 (3H, s, H-18), 1.17 (3H, s, H-29), 1.02 (3H, s, H-19), 0.96 (3H, s, H-30). ^{13}C NMR data (150 MHz, C_5D_5N) see Table 1.

*3.1.5. 20(*R*)-dammarane-3β,12β,20,25-tetrahydroxy-3β-O-β-D-glucopyranoside (**5**)*

White amorphous powder, Libermann-Burchard and Molish reactions were positive. Mp 213–215 °C. ESI-MS *m/z*: 639.9 $[M-H]^-$. ^1H NMR (400 MHz, C_5D_5N) δ: 3.93 (1H, s, H-12α), 3.38 (1H, s, H-3α), 1.99 (3H, s, H-28), 1.42 (3H, s, H-27), 1.41 (3H, s, H-26), 1.32 (3H, s, H-21), 1.01 (3H, s, H-29), 1.00 (3H, s, H-18), 0.95 (3H, s, H-19), 0.82 (3H, s, H-30). ^{13}C NMR data (150 MHz, C_5D_5N) see Table 1.

*3.1.6. β-Sitosterol (**6**)*

White amorphous powder. Mp 139–141 °C. ^{13}C NMR data (100 MHz, C_5D_5N) see Table 1.

Table 2
Inhibitory activities of compounds **1**–**8**.

Compounds	IC_{50} /(μmol·L^{-1})	
	α-Glucosidase	PTP1B
1	22.72 ± 0.79	27.23 ± 2.36
2	> 100	23.63 ± 5.09
3	15.42 ± 0.87	10.39 ± 0.21
4	6.26 ± 1.59	6.21 ± 0.21
5	0.22 ± 0.21	5.91 ± 0.38
6	69.41 ± 0.03	> 100
7	41.04 ± 0.34	18.99 ± 1.46
8	12.49 ± 1.22	13.38 ± 0.88
Acarbose	9.49 ± 0.18	–
Na_3VO_4	–	26.20 ± 1.78

*3.1.7. Oleanolic acid (**7**)*

White amorphous powder. Mp 308–310 °C. ESI-MS *m/z*: 457.7 $[M+H]^+$. ^1H NMR (400 MHz, C_5D_5N) δ: 5.28 (1H, brs, H-12), 3.22 (1H, dd, J = 10.2, 4.5 Hz, H-3), 1.13 (3H, s, H-29), 0.99 (3H, s, H-23), 0.93 (3H, s, H-27), 0.91 (3H, s, H-30), 0.90 (3H, s, H-26),0.77 (3H, s, H-24), 0.75 (3H, s, H-25). ^{13}C NMR data (100 MHz, C_5D_5N) see Table 1.

*3.1.8. 20(S)-protopanaxadiol (**8**)*

White amorphous powder. Mp 237–239 °C. ESI-MS *m/z*: 459.5 $[M-H]^-$. ^1H NMR (400 MHz, C_5D_5N) δ: 5.33 (1H, t, J = 7.2 Hz, H-24), 3.92 (1H, m, H-12α), 3.44 (1H, m, H-3α), 1.60 (3H, s, H-28), 1.59 (3H, s, H-21), 1.37 (3H, s, H-26), 1.17 (3H, s, H-27), 0.98 (3H, s, H-18), 0.95 (3H, s, H-29), 0.88 (3H, s, H-19), 0.83 (3H, s, H-30). ^{13}C NMR data (100 MHz, C_5D_5N) see Table 1.

The structures of eight known compounds (**1**–**8**) were shown in Fig. 1. They were white amorphous powder, and identified mainly by their corresponding NMR spectra (Table 1). The data obtained were compared with those reported in the literatures. The compounds were characterized as 20(*S*)-panaxadiol (**1**) (Cao, Fu, & Zhao, 2013), (20*S*,24*R*)-dammarane-20,24-epoxy- 3β,6α,12β,25-tetraol (**2**) (Wang, Bi, & Xu, 2013), 20(*R*)-dammarane-3β,12β,20,25-tetraol (**3**) (Ma & Yang, 2015), 20(*R*)-protopanaxadiol (**4**) (Ma & Yang, 2015), 20(*R*)-dammarane-3β,12β,20,25- tetrahydroxy-3β-*O*-β-*D*-glucopyranoside (**5**) (Ma & Yang, 2015), β-sitosterol (**6**), oleanolic acid (**7**) (Seebacher, Simic, Weis, Saf, & Kunert, 2003), 20(*S*)-protopanaxadiol (**8**) (Ma & Yang, 2015).

3.2. α-Glucosidase inhibition assay

α-Glucosidase and α-amylaseare are important enzymes in starch decomposition and intestinal absorption (Meng et al., 2016). The *in vitro* inhibitions against α-glucosidase of eight compounds were analyzed. As shown in Fig. 2A, seven samples displayed good inhibitory effects in a dose dependent manner. Among them, compounds **5** and **4** showed significant activities with IC_{50} values of 0.22, and 6.26 μmol/L, respectively, compared with IC_{50} (9.49 μmol/L) of acarbose in Table 2. The inhibitory activities (**5**: 86.93%; **4**: 67.82%, at 100 μmol/L). Compounds **1, 3, 7,** and **8** displayed moderate inhibition with IC_{50} values of 22.72, 15.42, 41.04, and 12.49 μmol/L, respectively. Compound **6** showed weak inhibitions at IC_{50} value of 69.41 μmol/L.

3.3. PTP1B inhibition assay

PTP1B plays a major role in modulating both insulin sensitivity and fuel metabolism, establishing it as a potential therapeutic target in the treatment of type 2 diabetes and obesity (Elchebly et al., 1999). The roles of compounds **1**–**8** against PTP1B were assessed using enzyme activity assay. It was indicated that **5** exhibited the highest inhibition effect (IC_{50} 5.91 μmol/L), its inhibitory

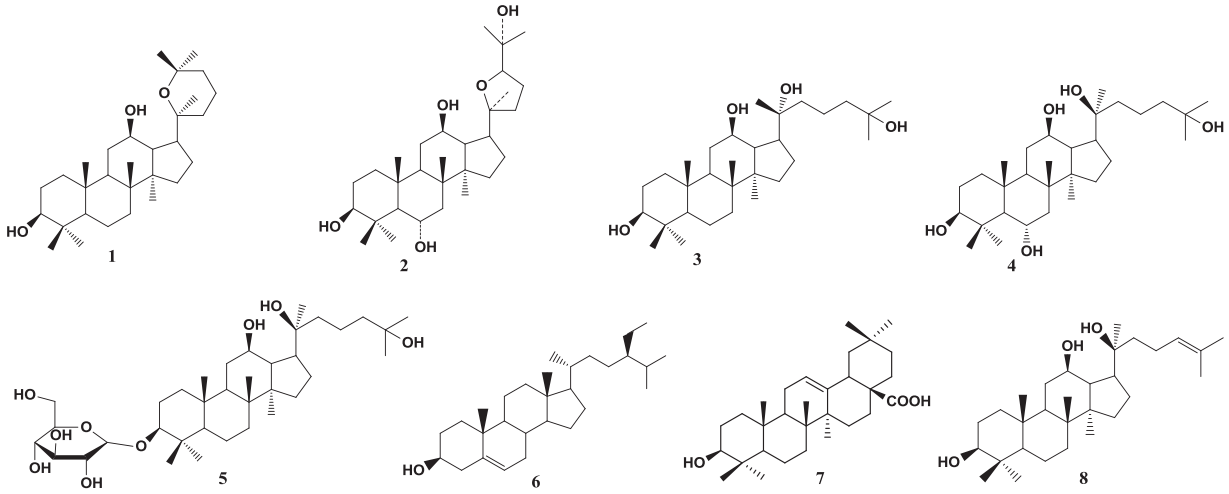

Fig. 1. Chemical structures of isolated compounds **1–8**.

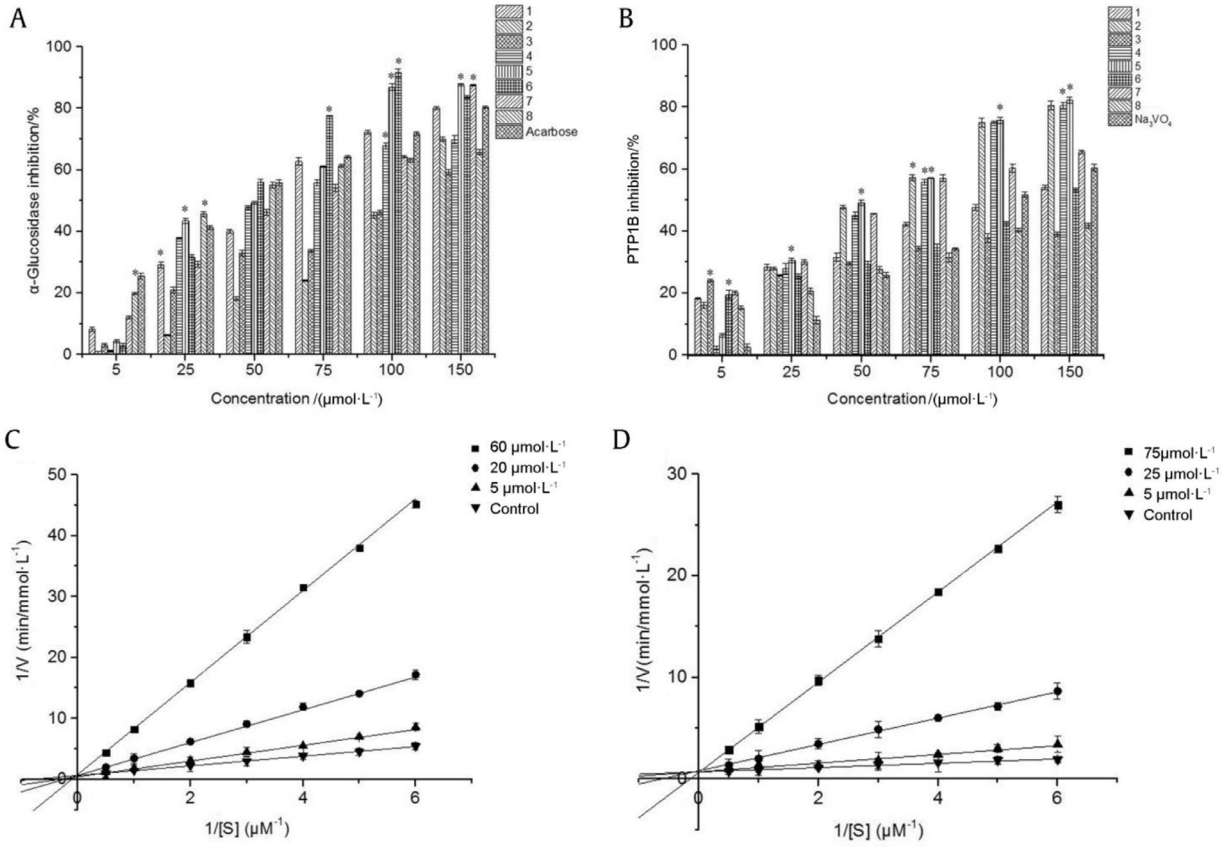

Fig. 2. Hypoglycemic activities of isolated compounds **1–8** (mean ± SD, $n = 3$). A: Inhibitory activities against a-glucosidase. B: Inhibitory activities against PTP1B. C: Lineweave–Burk double reciprocal curve of compound **5** against a-glucosidase. D: Lineweave–Burk double reciprocal curve of compound **5** against PTP1B. $^{*}P < 0.05$, denotes a significant effect, compared to acarbose or Na_3VO_4.

activity was 81.76% at 150 μmol/L. All the samples displayed good inhibitory effects in a dose-dependent manner (Fig. 2B). In Table 2, we also observed compounds **1, 6** and **7** showed significant activities with IC_{50} values of 10.77, 15.02, and 20.65 μmol/L, respectively, compared with IC_{50} (26.20 μmol/L) of Na_3VO_4. Compounds **2** and **3** displayed moderate inhibition at IC_{50} values of 37.46 and 49.12 μmol/L, respectively. **4** showed little inhibitions at IC_{50} value of 62.19 μmol/L.

3.4. Enzyme kinetic assay

The enzyme kinetics studies revealed that compound **5** inhibited α-glucosidase and PTP1B with characteristics typical of competitive inhibitors (Figs. 2C and D). It showed that, with increasing concentration of **5**, K_m increased significantly, whereas the V_{max} remained unaltered, which indicated they were competitive inhibitions for α-glucosidase and PTP1B.

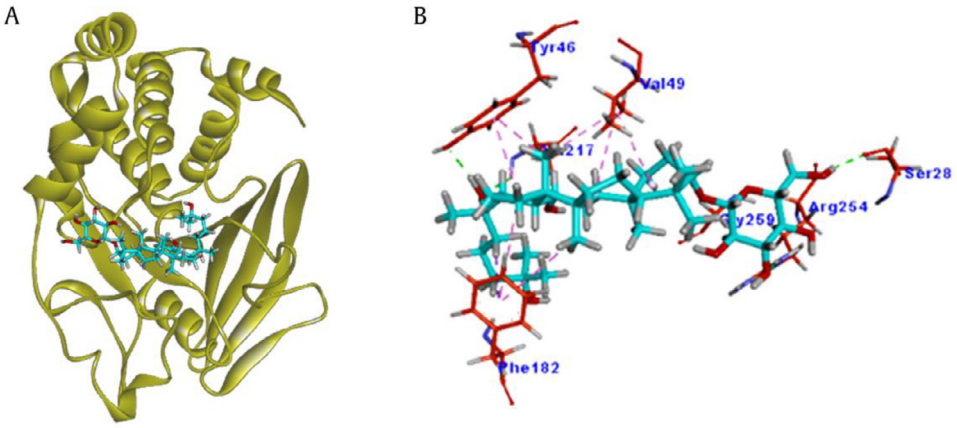

Fig. 3. Three-dimensional structure of compound **5** and PTP1B (A) and interaction between compound **5** and PTP1B (B).

3.5. Docking results of compound 5 and PTP1B

Molecular docking simulation of compound **5** to PTP1B space was discussed. The 12-OH and 20-OH interacted with Ala217 and Tyr46, respectively (Fig. 3). The 3′-OH and 6′-OH in glucose formed hydrogen bonds with Arg254 and Ser28. And the molecule was also by $\pi-\pi$ interaction with Val49, Phe182, Gly259, Val49 and Tyr46 of PTP1B. The inhibitor could bind to amino acid residues near the catalytic center, which may be the reason for its good PTP1B inhibition, thus achieving hypoglycemic activity. This result indicates that glucoside may be the better skeleton than the aglycone for the inhibition of PTP1B. The findings also confirmed that the number and substitutional position of OH in the skeleton were important in the PTP1B inhibition activity (Xiao et al., 2017).

By comparing the test compounds, it was found that the sequence of inhibitory activities were as following: **5** (IC_{50} = 5.91 μmol/L) > **4** (IC_{50} = 6.21 μmol/L) > **3** (IC_{50} = 10.39 μmol/L) > **8** (IC_{50} = 13.38 μmol/L) > **7** (IC_{50} = 18.99 μmol/L) > **2** (IC_{50} = 23.63 μmol/L) > **1** (IC_{50} = 27.23 μmol/L) > **6** (IC_{50} > 100 μmol/L), which suggested that the compound with more OH had better PTP1B inhibition activity.

4. Conclusion

In this work, we isolated eight compounds and identified their structures. To evaluate their hypoglycemic activity, the inhibitory activities were tested against α-glucosidase and PTP1B *in vitro*, which are directly related to the absorption or metabolism of glucose. Compound **5** is ginseng triterpenoid isolated from the acid hydrolysates of total saponins from *P. quinquefolius* for the first time. Further research demonstrated that **5** had significant inhibition activities. Based on the results, the discovery of active dammarane-type triterpenoids may provide an opportunity to develop *P. quinquefolius* as a potential source for type 2 diabetes treatment.

Declaration of Competing Interest

The authors declare no conflict of interests.

Acknowledements

This work was supported by the National Natural Science Foundation of China (No. 81602983).

References

Bai, M. S., Gao, J. M., Fan, C., Yang, S. X., Zhang, G., & Zheng, C. D. (2010). Bioactive dammarane-type triterpenoids derived from the acid hydrolysate of *Gynostemma pentaphyllum* saponins. *Food Chemistry, 119*(1), 306–310.

Cao, J. Q., Fu, P., & Zhao, Y. Q. (2013). Isolation and identification of a new compound from acid hydrolysate of saponin in stems and leaves of *Panax notoginseng*. *Chinese Traditional Herb Drugs, 44*(2), 137–140.

Cho, N., Shaw, J. E., Karuranga, S., Huang, Y., da Rocha Fernandes, J. D., & Ohlrogge, A. W. (2018). IDF Diabetes Atlas: Global estimates of diabetes prevalence for 2017 and projections for 2045. *Diabetes Research and Clinical Practice, 138*, 271–281.

Elchebly, M., Payette, P., Michaliszyn, E., Cromlish, W., Collins, S., & Loy, A. L. (1999). Increased insulin sensitivity and obesity resistance in mice lacking the protein tyrosine phosphatase-1B gene. *Science (New York, N.Y.), 283*, 1544–1548.

Fang, L. L., Cao, J. Q., Duan, L. L., Tang, Y., & Zhao, Y. (2014). Protein tyrosine phosphatase 1B (PTP1B) and α-glucosidase inhibitory activities of *Schisandra chinensis* (Turcz.) Baill. *Journal of Functional Foods, 9*, 264–270.

Imam, K. (2012). Clinical features, diagnostic criteria and pathogenesis of diabetes mellitus. *Advanced in Experimental Medicine and Biology, 771*, 340–355.

Liu, J. P., Tian, X., Liu, H. Y., Zhang, Q. H., Lu, D., Li, P. Y., et al. (2013). Two novel dammarane-type compounds from the leaves and stems of *Panax quinquefolium* L. *Journal of Asian Natural Products Research, 15*(9), 974–978.

Ma, L. Y., & Yang, X. W. (2015). Chemical constituents in acid hydrolysates of total saponins from stems and leaves of *Panax ginseng*. *Chinese Traditional Herb Drugs, 46*(27), 2522–2533.

Meng, Y., Su, A., Yuan, S., Zhao, H., Tan, S., Hu, C., et al. (2016). Evaluation of total flavonoids, myricetin, and quercetin from *Hovenia dulcis* Thunb. as inhibitors of α-amylase and α-glucosidase. *Plant Food for Human Nutrition, 71*(4), 444–449.

Qi, L. W., Wang, C. Z., & Yuan, C. S. (2010). American ginseng: Potential structure-function relationship in cancer chemoprevention. *Biochemical Pharmacology, 80*(7), 947–954.

Seebacher, W., Simic, N., Weis, R., Saf, R., & Kunert, O. (2003). Complete assignments of ^{1}H and ^{13}C NMR resonances of oleanolic acid, 18α-oleanolic acid, ursolic acid and their 11-oxo derivatives. *Magnetic Resonance in Chemistry, 41*(8), 636–638.

Tao, Y., Zhang, Y., Cheng, Y., & Wang, Y. (2013). Rapid screening and identification of α-glucosidase inhibitors from mulberry leaves using enzyme-immobilized magnetic beads coupled with HPLC/MS and NMR. *Biomedical Chromatography, 27*(2), 148–155.

Vuksan, V., Sievenpiper, J. L., Koo, V. Y., Francis, T., Beljan-Zdravkovic, U., Xu, Z., et al. (2000). American ginseng (*Panax quinquefolius L*) reduces postprandial glycemia in nondiabetic subjects and subjects with type 2 diabetes mellitus. *Archives of Internal Medicine, 160*(7), 1009–1013.

Wang, J. H., Lia, W., Sha, Y., Tezuka, Y., Kadota, S., & Li, X. (2001). Triterpenoid saponins from leaves and stems of *Panax quinquefolium* L. *Journal of Asian Natural Products Research, 3*(2), 123–130.

Wang, P., Bi, X. L., & Xu, J. (2013). Synthesis and anti-tumor evaluation of novel 25-hydroxy protopanaxadiol analogs incorporating natural amino acids. *Steroids, 78*(2), 203–309.

Xiao, T., Guo, Z., Sun, B., & Zhao, Y. (2017). Identification of anthocyanins from four kinds of berries and their inhibition activity to α-glycosidase and protein tyrosine phosphatase 1B by HPLC-FT-ICR MS/MS. *Journal of Agricultural and Food Chemistry, 65*(30), 6211–6221.

Xu, J., Cao, J. Q., Yue, J. Y., Zhang, X. S., & Zhao, Y. Q. (2018). New triterpenoids from acorns of *Quercus liaotungensis* and their inhibitory activity against α-glucosidase, α-amylase and protein-tyrosine phosphatase 1B. *Journal of Functional Foods, 41*, 232–239.